

1 **Phylogenomic comparative methods: accurate evolutionary inferences in the presence of**  
2 **gene tree discordance**

5 Mark S. Hibbins<sup>1,2</sup>, Lara C. Breithaupt<sup>2,3</sup>, and Matthew W. Hahn<sup>2,4</sup>

8 <sup>1</sup>Department of Ecology and Evolutionary Biology, University of Toronto, Toronto, ON, CA  
9 M5S 3B2

10 <sup>2</sup>Department of Biology and <sup>4</sup>Department of Computer Science, Indiana University,  
11 Bloomington, IN 47405

14 <sup>3</sup>Department of Computer Science, Duke University, Durham, NC 27710

17

18

19

20

21

22

23

24

25

26

27

28

29

30

31

32 **Abstract**

33

34 Phylogenetic comparative methods have long been a mainstay of evolutionary biology,  
35 allowing for the study of trait evolution across species while accounting for their common ancestry.  
36 These analyses typically assume a single, bifurcating phylogenetic tree describing the shared  
37 history among species. However, modern phylogenomic analyses have shown that genomes are  
38 often composed of mosaic histories that can disagree both with the species tree and with each  
39 other—so-called discordant gene trees. These gene trees describe shared histories that are not  
40 captured by the species tree, and therefore that are unaccounted for in classic comparative  
41 approaches. The application of standard comparative methods to species histories containing  
42 discordance leads to incorrect inferences about the timing, direction, and rate of evolution. Here,  
43 we develop two approaches for incorporating gene tree histories into comparative methods: one  
44 that constructs an updated phylogenetic variance-covariance matrix from gene trees, and another  
45 that applies Felsenstein's pruning algorithm over a set of gene trees to calculate trait histories and  
46 likelihoods. Using simulation, we demonstrate that our new approaches generate much more  
47 accurate estimates of tree-wide rates of trait evolution than standard methods. We apply our  
48 methods to two clades of the wild tomato genus *Solanum* with varying rates of discordance,  
49 demonstrating the contribution of gene tree discordance to variation in a set of floral traits. Our  
50 new approaches have the potential to be applied to a broad range of classic inference problems in  
51 phylogenetics, including ancestral state reconstruction and the inference of lineage-specific rate  
52 shifts.

53

54 **Significance statement**

55

56 Phylogenetic comparative methods allow for the study of trait evolution between species  
57 by accounting for their shared evolutionary history. These methods usually assume that species  
58 relationships can be described by a single tree. However, different parts of the genome can have  
59 their own independent evolutionary histories that can disagree with each other. If these disagreeing  
60 histories contribute to trait evolution over time, standard comparative methods can be misled. In  
61 this work, we developed two new approaches to phylogenetic comparative methods that account  
62 for this variation in histories across the genome. We used these methods to estimate more accurate  
63 rates of floral trait evolution in wild tomatoes. Our work opens new approaches for the study of  
64 trait evolution among species.

65  
66  
67  
68  
69  
70  
71  
72  
73  
74  
75  
76  
77

78 **Introduction**

80 A major goal of evolutionary biology is to understand how and why traits vary among  
81 species. One of the major sources of this variation is common ancestry. If left unaccounted for,  
82 this shared history can lead to pseudoreplication and spurious trait correlations (Felsenstein 1985).  
83 Phylogenetic comparative methods have been developed to account for shared history, enabling  
84 more accurate inferences about the tempo and mode of trait evolution (Harvey and Pagel 1991).  
85 With the statistical toolkit offered by phylogenetic comparative methods, researchers can ask  
86 questions about the rate at which traits evolve, whether these rates have changed over time or in  
87 different lineages, what traits may have looked like in ancestral or extinct lineages, and whether  
88 trait shifts are correlated with historical or environmental factors (Martins and Hansen 1996;  
89 Garamszegi 2014; Adams and Collyer 2018; Revell and Harmon 2022).

90 In classic comparative methods, common ancestry among species is accounted for by using  
91 a single species phylogeny. However, genome-scale analyses of phylogenetic history have  
92 revealed that individual loci can have their own independent histories (Pollard et al. 2006; White  
93 et al. 2009; Fontaine et al. 2015; Pease et al. 2016; Novikova et al. 2016; Copetti et al. 2017; Wu  
94 et al. 2018; Edelman et al. 2019; Vanderpool et al. 2020). The result is gene tree discordance—the  
95 disagreement of trees at individual loci both with each other and with the species phylogeny. Gene  
96 tree discordance has important implications for phylogenetic comparative methods because  
97 discordant gene trees contain branches that are not present in the species phylogeny. Evolution  
98 along such discordant branches can result in trait similarity among species with no shared history  
99 in the species tree (Figure 1). Such patterns of trait variation can mislead standard phylogenetic  
100 comparative methods, particularly by resulting in overestimates of the number of trait transitions  
101 or the rate of trait evolution (Hahn and Nakhleh 2016; Mendes and Hahn 2016; Mendes et al. 2018;  
102 Hibbins et al. 2020; Wang et al. 2021). This effect has been termed "hemiplasy," as single  
103 transitions on discordant gene trees can falsely resemble homoplasy when analyzed on the species  
104 tree (Avise and Robinson 2008).

105 Discordance is a concern for evolutionary inference because it has biological causes that  
106 cannot be overcome by addressing technical errors or by increasing species sampling (Degnan and  
107 Rosenberg 2009). Two primary causes of discordance, incomplete lineage sorting (ILS) and  
108 introgression, have different effects on gene tree frequencies and branch lengths and are therefore  
109 expected to bias comparative methods in different ways. ILS, a stochastic process that depends on  
110 species tree internal branch lengths and population sizes, generates symmetry in the frequencies  
111 of possible discordant gene trees (Hudson 1983; Pamilo and Nei 1988). Therefore, higher amounts  
112 of ILS lead to broad increases in the occurrence of hemiplasy across multiple possible incongruent  
113 trait patterns (Guerrero and Hahn 2018; Mendes et al. 2018). Introgression is a process of historical  
114 hybridization and back-crossing that, while widespread in modern phylogenomic datasets (Mallet  
115 et al. 2016; Taylor and Larson 2019; Dagitlis et al. 2022), is often more limited to specific pairs of  
116 taxa. In particular, post-speciation introgression between non-sister lineages leads to an excess of  
117 gene trees grouping those lineages as sister (Reich et al. 2009; Green et al. 2010; Durand et al.  
118 2011; Patterson et al. 2012). This pattern should result in an excess of trait-sharing for the species  
119 involved in introgression compared to the species not exchanging genes (Hibbins et al. 2020;  
120 Hibbins and Hahn 2021; Wang et al. 2021).

123 While some progress has been made in accounting for discordance in the evolution of  
124 discrete traits, especially in nucleotide models (De Maio et al. 2013; De Maio et al. 2015;  
125 Schrempf et al. 2016; Ogilvie et al. 2017; Schrempf et al. 2019), many classic phylogenetic  
126 comparative methods remain unable to account for gene tree discordance when analyzing  
127 quantitative traits. The approaches required to improve these methods will depend on the question  
128 being asked. Some tasks, such as maximum-likelihood estimation of the rate of trait evolution  
129 under Brownian motion ( $\sigma^2$ ) (e.g. Garland and Ives 2000; O'Meara et al. 2006) or phylogenetic  
130 regression (Grafen 1989), depend on the specification of a matrix that describes the trait variances  
131 and covariances expected from the species phylogeny (often denoted  $\mathbf{C}$ ). Other comparative  
132 approaches, such as ancestral state reconstruction (Pagel 1999) and inference of lineage-specific  
133 rate shifts (Alfaro et al. 2009), can require more sophisticated approaches that calculate state  
134 probabilities on different parts of a phylogeny; one such approach is to use Felsenstein's pruning  
135 algorithm applied to a species tree with specified branch lengths (Felsenstein 1973). Mendes et al.  
136 (2018) showed that failing to account for discordance can bias estimates of  $\sigma^2$  upwards and can  
137 lead to falsely inflated numbers of trait-mean transitions. In general, the development of a  
138 comparative framework incorporating gene tree discordance would lead to more accurate  
139 evolutionary inferences in a wide variety of systems with ILS and/or introgression, across a wide  
140 variety of approaches for making inferences about quantitative traits.

141  
142 Here, we demonstrate the utility of an updated *phylogenomic* comparative framework,  
143 using two distinct approaches to incorporate the summed history of concordant and discordant  
144 gene trees into evolutionary inference. In the first approach, we show how to construct an updated  
145 phylogenetic variance/covariance matrix (which we denote  $\mathbf{C}^*$ ) to include the covariances  
146 introduced by discordant gene trees. We provide a new R package, *seastaR*, that can construct this  
147 updated matrix for any number of species, either by summing the internal branches of an input set  
148 of gene trees or by calculating expected gene tree internal branches from an input species tree  
149 using the multispecies coalescent model. We show how estimates of the evolutionary rate are made  
150 more accurate by using  $\mathbf{C}^*$ , and suggest how this updated matrix can be passed to other available  
151 software packages to make multiple evolutionary inferences more robust to discordance. In the  
152 second approach, we develop a method for applying the pruning algorithm over a set of gene trees  
153 to return the likelihood of an observed trait across species. Using a pilot implementation of this  
154 approach for a rooted three-species tree, we show how it can be used to accurately estimate the  
155 rate of quantitative trait evolution. Although currently limited to a smaller number of species, this  
156 latter approach has the potential to perform more complicated comparative inferences in the  
157 presence of discordance. Finally, we apply our approaches to empirical morphological data from  
158 wild tomatoes (Haak et al. 2014), finding a greater discrepancy between species tree and gene tree  
159 rate estimates in a clade with a higher rate of gene tree discordance. Overall, our new approaches  
160 pave the way towards more accurate evolutionary inferences in the presence of gene tree  
161 discordance.

162

## 163 **Methods**

164

### 165 *Building a phylogenetic variance/covariance matrix from data with discordance*

166

167 As previously discussed, one of the most common ways that phylogeny is incorporated  
168 into comparative analyses is by constructing a phylogenetic variance/covariance matrix,  $\mathbf{C}$ . This

169 square matrix has rows and columns corresponding to the number of taxa in the phylogeny, with  
 170 the diagonal elements containing the expected trait variances for each species and the off-diagonal  
 171 elements containing the expected trait covariances between each species pair. Considering three  
 172 species with the relationship ((A,B),C) (Figure 2A), the standard covariance matrix has the  
 173 following form:

$$174 \quad \mathbf{C} = \begin{bmatrix} \text{Var}(A) & \text{Cov}(AB) & 0 \\ \text{Cov}(BA) & \text{Var}(B) & 0 \\ 0 & 0 & \text{Var}(C) \end{bmatrix} \quad Eq\ 1$$

175 Trait covariances arise from shared internal branches in the phylogeny. As only species A and B  
 176 share an internal branch in the species tree, the other two species pairs have no expected  
 177 covariance.

178 In contrast, if we consider the gene trees that are generated by the species tree in Figure  
 179 2A, the two discordant gene trees contain internal branches shared by pairs B-C and A-C.  
 180 Discordance due to ILS generates all three possible topologies for this species tree, so all off-  
 181 diagonal entries in the covariance matrix should have non-zero values (Mendes et al. 2018). We  
 182 are interested in estimating this updated covariance matrix, which we denote  $\mathbf{C}^*$ :

$$185 \quad \mathbf{C}^* = \begin{bmatrix} \text{Var}(A) & \text{Cov}(AB) & \text{Cov}(AC) \\ \text{Cov}(BA) & \text{Var}(B) & \text{Cov}(BC) \\ \text{Cov}(CA) & \text{Cov}(CB) & \text{Var}(C) \end{bmatrix} \quad Eq\ 2$$

186 To construct  $\mathbf{C}^*$ , we provide the R package *seastaR*. *seastaR* uses two approaches for estimating  
 187  $\mathbf{C}^*$ , both following the same principle: each gene tree topology contributes an internal branch  
 188 which, after being weighted by that tree's expected frequency, fills an off-diagonal entry in the  
 189 covariance matrix (Figure 2A). Each gene tree also contributes its total height, weighted by  
 190 frequency, to the expected trait variances for each species. Both approaches assume that each  
 191 individual gene tree contributes equally to trait variation among species (i.e. the effect size of  
 192 mutations that affect trait variation does not differ on average among loci). We also assume that  
 193 loci contributing to trait variation follow the same distribution of tree topologies as the genome at  
 194 large, so the specified loci do not have to be explicitly related to the trait in question.

195 The first approach for estimating  $\mathbf{C}^*$ , *trees\_to\_vcv*, constructs this matrix from a list of  
 196 provided gene trees (with branch lengths) and their observed frequencies. The method works by  
 197 obtaining all the internal branch lengths present in each gene tree, as well as the height of each  
 198 gene tree, and averaging them to get  $\mathbf{C}^*$ . A major advantage of this approach is that it can easily  
 199 account for both ILS and introgression as sources of gene tree discordance, as the effects of both  
 200 are captured in the distribution of observed gene tree topologies and branch lengths. On the other  
 201 hand, individual gene trees may be inferred with error, making their branch lengths and frequencies  
 202 less reliable. If accurately estimated gene trees are unavailable, our second approach,  
 203 *get\_full\_matrix*, constructs  $\mathbf{C}^*$  solely from an input species tree in coalescent units. This method  
 204 breaks the input phylogeny down into each possible triplet, and for each triplet uses expectations  
 205 from the multispecies coalescent model to calculate the expected internal branches and frequencies  
 206 for each possible gene tree (see Mendes et al. 2018). For an exemplar five-taxon tree specified in

210 coalescent units, we compared the standard  $\mathbf{C}$  matrix to a  $\mathbf{C}^*$  matrix computed using  
211 `get_full_matrix` (Figure 2B). The test tree has three internal branches, each of length of 0.1  
212 coalescent units. Given these branch lengths, we expect 60% of trees to be discordant for each of  
213 these three branches, meaning that only 40% of gene trees will have (for instance) the clade  
214 containing species 5 and 4 sister to the clade containing species 3 and 2. As expected,  $\mathbf{C}^*$  contains  
215 covariance entries for species pairs that do not share an internal branch in the species tree, but that  
216 share internal branches in at least one discordant gene tree (Figure 2B). In addition, the sister  
217 lineages in the species tree have smaller covariances in  $\mathbf{C}^*$  than in  $\mathbf{C}$ , because they do not share an  
218 internal branch in many discordant trees.  
219

220 Our package, *seastaR*, contains several other utilities, including a parser for an input set of  
221 estimated gene trees, a simulator that can simulate trait evolution using  $\mathbf{C}^*$ , and a function to obtain  
222 the maximum-likelihood estimate of  $\sigma^2$  using  $\mathbf{C}^*$  (see Results). Also note that, although not  
223 currently implemented, *seastaR* could be extended to construct  $\mathbf{C}^*$  from an input species network  
224 specified in coalescent units, using expectations from the multispecies network coalescent model  
225 (Hibbins and Hahn 2021).  
226

## 227 *Calculating trait likelihoods over a set of gene trees using Felsenstein’s pruning algorithm*

  
228

229 Updating the phylogenetic variance/covariance matrix provides a straightforward solution  
230 to accounting for gene tree discordance that works for several important inference tasks in  
231 comparative methods. However, many questions require more sophisticated models that do not  
232 have straightforward solutions making use of this matrix. For these questions, the field would  
233 benefit from a general approach to calculating likelihoods given a set of gene trees and a model of  
234 trait evolution. Our solution makes use of Felsenstein’s pruning algorithm (Felsenstein 1973), a  
235 dynamic programming algorithm that calculates probabilities for a set of character states across all  
236 nodes in a phylogeny. A tree-wide likelihood can be calculated from the probabilities at the root,  
237 which can be used in conjunction with numerical optimization methods to estimate model  
238 parameters.  
239

240 We developed an approach to apply the pruning algorithm to a specified set of gene trees,  
241 rather than to a single tree. This approach is implemented in C++ and draws heavily on the  
242 infrastructure of *CAFE* (Hahn et al. 2005, Mendes et al. 2020), a program that uses the pruning  
243 algorithm to calculate likelihoods for a birth-death model of gene family evolution. We make  
244 several modifications based on the methods presented in Boucher and Démery (2016) and  
245 implemented in *CAGEE* (<https://github.com/hahnlab/CAGEE>) that allow *CAFE*’s implementation  
246 of the pruning algorithm to be applied to continuous traits rather than integer counts of gene  
247 families (see also Bertram et al. 2022). First, the pruning algorithm requires a vector of possible  
248 discrete character states over which probabilities can be calculated. To obtain this vector from an  
249 observed continuous trait, we take the range  $(-2(\max(|\mathbf{X}|), 2(\max(|\mathbf{X}|)))$  where  $\mathbf{X}$  is the vector  
250 of observed characters for each species. The vector of character states is then filled with 100  
251 equidistant steps from the lower bound to the higher bound. Second, we need to assign probabilities  
252 to all the character states at the tips of the phylogeny, so that the pruning algorithm has a place to  
253 start. This is straightforward for integer count data, as the observed value can simply be assigned  
254 a probability of 1 at the tip. However, for continuous traits it will often be the case that none of the  
255 values in our discretized trait vector exactly match the observed values at the tips. Therefore, we

256 implement an approach that distributes the probability at the tip over the two states in the  
 257 discretized vector closest to each of the observed values, proportional to how distant they are from  
 258 the observed value (Equation 18 in the appendix of Boucher and Démery 2016). Third, to calculate  
 259 the transition probability between each pair of discretized trait values over a branch in the  
 260 phylogeny, we use the Brownian motion model. The probability density for Brownian motion is:  
 261

$$262 p(x, x_0, t) = \frac{1}{\sqrt{2\pi t}\sigma} e^{-\frac{(x-x_0)^2}{2\sigma^2 t}}$$

263 *Eq 3*

264 where  $x_0$  is the initial trait value,  $x$  is the trait value after time  $t$ , and  $\sigma^2$  is the evolutionary rate per  
 265 unit time. With these methods in place, we can apply the standard pruning algorithm to an  
 266 individual tree with observed character states and a specified  $\sigma^2$  value.  
 267

268 To estimate a single likelihood over a set of gene trees, we initially apply the standard  
 269 pruning algorithm to each gene tree individually. Like the covariance matrix approach, we assume  
 270 that individual loci contribute equally to trait variation among species, and that trait loci follow the  
 271 same distribution of tree topologies as the genome at large. These gene trees with branch lengths  
 272 are given to the method directly, and must be ultrametric. Any set of trees can be specified, but the  
 273 manner in which they are specified will depend on the size of the species tree (i.e. number of tips).  
 274 For a large species tree, individual gene trees can be inferred or predicted by theory, similarly to  
 275 the two approaches used by *seastaR*. Because it may not be possible to sample every possible  
 276 topology, we recommend sampling a reasonable number of individual gene trees (see Discussion).  
 277 For a small species tree, the most efficient approach will be to specify one tree for each possible  
 278 topology, along with its frequency. Again, the branch lengths and frequencies of each tree topology  
 279 can be averaged from a set of inferred trees or predicted from theory. The total likelihood is then  
 280 calculated as:  
 281

$$282 L = \sum_{\tau} f(\tau_i) \left( -\log \left( \max(\mathbf{p}_{\tau_i}) \right) \right)$$

283 *Eq 4*

284 where  $\tau$  is the set of gene trees,  $f(\tau_i)$  is the frequency of gene tree  $i$ , and  $\mathbf{p}_{\tau_i}$  is the vector of  
 285 character state probabilities at the root for gene tree  $i$ . In words: we obtain a partial negative log-  
 286 likelihood for each individual gene tree, these partial likelihoods are then weighted by each gene  
 287 tree's observed frequency, and finally the weighted partial likelihoods are summed together to  
 288 produce the total likelihood (Figure 3).  
 289

290 A major advantage of the pruning algorithm method is that maximum-likelihood inference  
 291 can be used to estimate parameters for a wide variety of models. In addition, like the *trees\_to\_vcv*  
 292 method of *seastaR*, this approach can easily handle introgression events if the signals of  
 293 introgression are contained in the specified gene trees, or if expected gene trees under the  
 294 multispecies network coalescent could be specified by the user. Currently, our implementation  
 295 uses the Nelder-Mead algorithm (Nelder and Mead 1965) to find the optimal Brownian motion  
 296 evolutionary rate parameter,  $\sigma^2$ . In the future, we would like the software to also perform more

297 sophisticated inferences, such as ancestral state reconstruction or lineage-specific rate shifts. Our  
298 approach could also be extended to any evolutionary model, not just Brownian motion.

299  
300 *Simulating complex traits with discordance*  
301

302 To demonstrate the utility of our new phylogenomic comparative approaches, we used  
303 simulations to evaluate their performance on a simple inference task: estimating the evolutionary  
304 rate parameter,  $\sigma^2$ . We simulated traits from a phylogenetic history with increasing rates of gene  
305 tree discordance by making random draws from a multivariate normal distribution (where  $\mathbf{C}^*$   
306 specifies the covariance structure). This simulation approach assumes an infinitesimal contribution  
307 to the trait from all genomic loci, an approximation that holds reasonably well for many complex  
308 quantitative traits. For each simulated dataset, we applied both standard inference of  $\sigma^2$  using the  
309 species tree and our updated inferences that account for gene tree discordance. See the  
310 Supplementary Methods for the exact conditions and parameters used in our simulations.  
311

312 We simulated our traits under the model parameterization of Mendes et al. (2018). Levels  
313 of discordance in this model are altered by changing the effective population size,  $N$ , allowing us  
314 to increase the level of discordance by increasing  $N$ . The equations for trait variances and  
315 covariances are also scaled by  $N$ , such that branch lengths in units of absolute time are divided by  
316  $2N$ . The evolutionary rate is a compound parameter,  $2N\mu\sigma_M^2$ , where  $\mu$  is the mutation rate and  $\sigma_M^2$   
317 is the variance in mutational effect sizes. A consequence of this formulation of the evolutionary  
318 rate is that the true rate used to simulate the data increases as we increase the rate of discordance  
319 by increasing  $N$ . This model is akin to the one shown in Figure 1B, in which mutations occur on  
320 gene tree branches with normally distributed effect sizes. Given enough mutations and enough  
321 time, these cumulative effects resemble Brownian motion of trait means along each lineage (Figure  
322 1C; Mendes et al. 2018).  
323

324 *Data availability*  
325

326 Source code and analysis scripts related to *seastaR* and the covariance matrix method can  
327 be found in <https://github.com/larabreithaupt/seastaR>. Code and scripts related to the pruning  
328 algorithm method can be found in <https://github.com/mhibbins/genetreepruningalg>.  
329

330 **Results**  
331

332 *Phylogenomic comparative approaches yield more accurate evolutionary rate estimates in the  
333 presence of discordance*  
334

335 We applied both of our new phylogenomic comparative approaches to data simulated with  
336 discordance in order to evaluate their accuracy in estimating the evolutionary rate parameter,  $\sigma^2$ .  
337 For the approach that uses the updated the variance/covariance matrix,  $\mathbf{C}^*$ , we use the maximum-  
338 likelihood estimator of  $\sigma^2$ :  
339

$$340 \hat{\sigma}^2 = \frac{[\mathbf{X} - E(\mathbf{X})]^T \mathbf{C}^{-1} [\mathbf{X} - E(\mathbf{X})]}{n}$$

341 *Eq 5*

342 (O'Meara et al. 2006), where  $\mathbf{X}$  is the vector of observed trait values at the tips,  $\mathbf{C}$  is the  
343 phylogenetic variance-covariance matrix, and  $n$  is the number of tips.  $E(\mathbf{X})$  is the vector containing  
344 the expected trait value at the root, calculated as follows:

345

$$346 \quad E(\mathbf{X}) = \mathbf{1}[(\mathbf{1}^T \mathbf{C}^{-1} \mathbf{1})^{-1} (\mathbf{1}^T \mathbf{C}^{-1} \mathbf{X})] \quad Eq \ 6$$

347

348 Where  $\mathbf{1}$  is a column vector of ones of size  $n \times 1$ . To account for gene tree discordance with this  
349 estimator, we simply use  $\mathbf{C}^*$  in place of  $\mathbf{C}$  in equations 5 and 6. We have implemented this method  
350 in *seastaR* to allow users to estimate  $\sigma^2$ . For this approach, we simulated 1000 trait datasets for  
351 each condition of increasing gene tree discordance, estimating  $\sigma^2$  using both  $\mathbf{C}$  and  $\mathbf{C}^*$  for each  
352 dataset.

353

354 For the approach using the pruning algorithm, we implemented the Nelder-Mead  
355 optimization algorithm. Given a set of input gene trees and tree frequencies, our optimization  
356 approach proposes a new value of  $\sigma^2$  in each iteration, returning a single likelihood value over the  
357 set of gene trees each time; the optimal value of  $\sigma^2$  is the one that maximizes this total likelihood.  
358 Owing to longer computation times, we simulated 100 trait datasets for each set of parameters with  
359 this method, using either a single tree specified (the species tree) or multiple trees specified (the  
360 gene trees).

361

362 As expected, we found that increasing the level of discordance results in an increasingly  
363 upward bias in estimates of the evolutionary rate from the species tree (Figure 4, green lines). As  
364 there are no internal branches in the species tree that can explain the increased trait covariances  
365 between non-sister taxa, such methods must propose a higher evolutionary rate to explain the data.  
366 In contrast, we found that both the covariance matrix approach (i.e.  $\mathbf{C}^*$ ; Figure 4A) and pruning  
367 algorithm approach (Figure 4B) yielded more accurate evolutionary rate estimates, ones that  
368 closely tracked the true population-scaled evolutionary rate as the level of discordance increased.  
369 Both phylogenomic comparative approaches can model the increased covariances generated by  
370 the increasing frequencies of discordant gene trees. As can be observed, both approaches tend to  
371 slightly underestimate the true evolutionary rate, but they are much closer to the true value than  
372 standard species tree estimates, especially at higher rates of discordance.

373

374 *Phylogenomic comparative approaches are robust to the effects of gene tree estimation error*

375

376 In empirical datasets, it is reasonable to expect gene trees to be estimated with some degree  
377 of error, especially in the limits of short sequence length (such as ultra-conserved elements), long  
378 periods of evolutionary divergence, or high rates of sequencing error. In general, these sources of  
379 technical error should not be biased towards specific lineages, so their effect should be to cause  
380 general overestimation of gene tree discordance. This may in turn result in lower evolutionary rate  
381 estimates when using our approaches, as they might “overcorrect” the problem. More generally,  
382 we were concerned that increasing the rate of discordance might always lead to a lower  
383 evolutionary rate estimate, regardless of the true history that generated the data. Such behavior  
384 would present a potential problem for the application of our approaches to empirical datasets.

385

386 To address these concerns, we simulated traits from gene trees under a single, fixed rate of  
387 gene tree discordance (of approximately 15%) using the methods described in the previous section.

388 We then applied our approaches to estimating  $\sigma^2$  to this dataset, varying the specified rate of gene  
389 tree discordance from 0 (in which case we used the standard species tree inference) to  
390 approximately 60%. In contrast to our initial concerns, we found that in both the covariance matrix  
391 (Figure 5A) and pruning algorithm (Figure 5B) approaches: 1) the effect of mis-specifying the rate  
392 of gene tree discordance is relatively small compared to the effect of using the species tree in place  
393 of gene trees; 2) increasing the specified rate of gene tree discordance leads to a small increase,  
394 rather than decrease, in the estimated evolutionary rate, but still closely tracked the true value. This  
395 latter effect may occur because increasing the specified rate of gene tree discordance requires  
396 branch lengths to be scaled down in accordance with  $N$ , resulting in less proposed time over which  
397 evolutionary changes can occur. Overall, these results suggest that gene tree estimation error  
398 should not be a major concern for our approaches, as long as the correct set of tree topologies is  
399 specified.

400

401 *Rate estimates for floral traits in the wild tomato clade Solanum are consistent with evolution on*  
402 *discordant gene trees*

403

404 Our simulations show that when traits evolve on discordant gene trees, standard species  
405 tree approaches tend to greatly overestimate the true value, while our gene tree approaches slightly  
406 underestimate the true value but are much more accurate. The degree of discrepancy between  
407 species tree and gene tree approaches grows larger as the rate of discordance increases. To further  
408 test these expectations and to highlight the application of our methods to empirical data, we  
409 estimated the evolutionary rates of several floral traits (anther length, corolla diameter, and stigma  
410 length) measured in wild tomatoes (*Solanum*) (Haak et al. 2014). We obtained the time-scaled  
411 phylogeny of this clade from Pease et al. (2016) and converted from time in years to coalescent  
412 units assuming  $N = 100,000$  and one generation every two years (Hamlin et al. 2020). We then  
413 pruned the phylogenetic tree into high and low ILS triplets, each consisting of three taxa. The high  
414 ILS group consisted of the following accessions (IDs from the Tomato Genetics Resource Center):  
415 *S. galapagense* LA0436, *S. cheesmaniae* LA3124, and *S. pimpinellifolium* LA1269; the low ILS  
416 group consisted of *S. pennellii* LA3778, *S. pennellii* LA0716, and *S. pimpinellifolium* LA1589.  
417 Based on the internal branch lengths in coalescent units, the high ILS and low ILS triplets had  
418 expected rates of discordance of approximately 47% and 0.9%, respectively. These rates  
419 correspond to the rates of discordance seen in empirically estimated gene trees in Pease et al.  
420 (2016). Based on our simulation results, if discordant gene trees contribute to tomato floral trait  
421 variation, we should see a greater discrepancy between species tree methods and our gene tree  
422 methods in the high ILS triplet.

423

424 In both of our approaches, we used the multispecies coalescent model to calculate the  
425 expected gene tree frequencies and branch lengths in each triplet. For the covariance matrix  
426 method, we used these expectations to construct the covariance matrix  $C^*$  for each triplet using  
427 the `get_full_matrix()` method. For the pruning algorithm method, we specified a representative  
428 gene tree of each of the possible topologies with expected branch lengths, and weighted each tree  
429 by its expected frequency. For both methods, we used the standard approach of specifying a single  
430 species tree and our gene tree approaches to estimate the evolutionary rate using the mean trait  
431 values within each accession if multiple individuals were measured.

432

433 In line with our expectations, rate estimates obtained from standard species tree approaches  
434 are much higher than those obtained from both of our gene tree methods in the high ILS triplet,  
435 for all three traits (Figure 6). The discrepancy is much smaller in the low ILS triplets (Figure 6).  
436 The bias due to discordance was very large for the estimates obtained from the covariance matrix  
437 method in *seastaR* (Figure 6A), where the species tree rate estimates were several orders of  
438 magnitude higher than the gene tree estimates in the high ILS triplet. This is consistent with our  
439 simulation finding that the estimated evolutionary rate is more biased under discordance when  
440 using covariance methods (Figure 4A). Even when accounting for gene tree discordance, the rate  
441 estimates obtained from the covariance matrix method were substantially higher than those  
442 obtained from the pruning algorithm method (compare Figure 6A and 6B). This discrepancy can  
443 be explained by flat/undefined likelihood surfaces for the proposed values of  $\sigma^2$  (Supplementary  
444 Figure 1): the pruning algorithm method, which employs a likelihood search, reaches a likelihood  
445 plateau and does not propose further improvements, whereas the covariance matrix method uses  
446 the analytical likelihood estimator to obtain the maximum value, regardless of the shape of the  
447 likelihood surface. This problem may arise when a small number of taxa are studied, as less  
448 information is available to discern the rate of trait evolution. To help users evaluate this problem  
449 in their datasets, we have implemented a function for calculating trait likelihoods over a range of  
450 proposed  $\sigma^2$  values in *seastaR*. In this case, we believe the pruning algorithm estimates represent  
451 more biologically realistic rates of evolution.

452

453

## 454 Discussion

455

456 There has been much phylogenetic research focused on the accurate estimation of species  
457 trees in the face of gene tree discordance (e.g. Degnan and Rosenberg 2009; Bryant et al. 2012;  
458 Chifman and Kubatko 2014; Mirarab et al. 2014; Mendes and Hahn 2018; Zhang et al. 2018).  
459 Despite this focus on inferring trees in the face of discordance, standard phylogenetic comparative  
460 methods still rely on a single “resolved” tree to describe the shared history of species. Recent work  
461 has made it clear that, if only a single tree is used, gene tree discordance can shape trait variation  
462 and mislead comparative methods (e.g. Mendes et al. 2018; Hibbins et al. 2020). However, few  
463 solutions have been proposed to solve these problems, especially for quantitative traits evolving  
464 on clades containing discordance. Here, we have developed two approaches, which we refer to as  
465 *phylogenomic* comparative methods, that can incorporate gene tree discordance into comparative  
466 inference. One approach uses a more complete phylogenetic variance-covariance matrix that  
467 includes the covariance present in discordant gene trees. We have developed an R package,  
468 *seastaR*, for building this matrix using the frequencies and branch lengths of relevant gene trees.  
469 The second approach applies the pruning algorithm over a set of gene trees—concordant and  
470 discordant—to estimate likelihoods. Using simulation, we demonstrate that these methods  
471 generate more accurate evolutionary rate estimates for traits evolving in the presence of  
472 discordance, and are generally robust to the effects of gene tree estimation error. Finally, we  
473 demonstrate that empirical floral traits in the wild tomato clade *Solanum* are consistent with  
474 evolution on discordant gene trees, with the clade with a higher rate of gene tree discordance  
475 exhibiting a greater discrepancy in rate estimates between traditional approaches and our new  
476 methods.

477

478        Many phylogenetic comparative methods take the variance-covariance matrix,  $\mathbf{C}$ , as input  
479 (e.g. Pagel 1999; Housworth et al. 2004; O’Meara et al. 2006; Revell and Harmon 2008). Because  
480 of the wide use of  $\mathbf{C}$ , we anticipate that a more complete variance-covariance matrix,  $\mathbf{C}^*$ , will be  
481 easy to incorporate into many comparative analyses. The *seastar* package provides an easy way  
482 for users to generate  $\mathbf{C}^*$ , either from a set of specified gene trees or from a specified species tree  
483 (assuming a multispecies coalescent process). Here, we have demonstrated how  $\mathbf{C}^*$  can be used to  
484 obtain a maximum-likelihood estimate of the rate of quantitative trait evolution under Brownian  
485 motion, a method that is also implemented in *seastar*. One obvious extension of the use of  $\mathbf{C}^*$  is  
486 in phylogenetic generalized linear mixed models (PGLMMs), where the covariance matrix is often  
487 specified directly in packages such as *MCMCglmm* (Hadfield 2010). However, many popular  
488 packages for implementing comparative methods—such as *phytools* (Revell 2012), *ape* (Paradis  
489 and Schliep 2019), and *Geiger* (Pennell et al. 2014)—do not take a matrix directly, instead turning  
490 an input species tree into a matrix. Furthermore, they require a strictly bifurcating tree as input to  
491 construct a *phylo* class object. Integrating the ability to accept  $\mathbf{C}^*$  (or equivalent sets of gene trees)  
492 into these methods would enable a much larger array of inference tasks to take discordance into  
493 account.

494

495        The pruning algorithm is widely used in likelihood-based inference of phylogenetic trees  
496 (Felsenstein 1981) and for some applications in quantitative trait evolution (e.g. Hahn et al. 2005;  
497 FitzJohn 2012; Freckleton 2012; Ho and Ané 2014; Uyeda and Harmon 2014; Hiscox et al. 2016;  
498 Mitov et al. 2020). Our method using the pruning algorithm across a set of gene trees makes many  
499 of the same assumptions as previous implementations, but models each trait as the combined result  
500 of a large number of loci; these loci were represented in our calculations by a smaller number of  
501 exemplar gene tree topologies, each with the mean set of branch lengths for a given topology.  
502 Although it is not as straightforward to incorporate our method into other approaches as with  $\mathbf{C}^*$ ,  
503 because the pruning algorithm is a general method for calculating likelihoods, it has enormous  
504 potential to be applied to a wide variety of inference problems. As trees get larger, the  
505 computational cost of the matrix operations in equations 5 and 6 grows exponentially with the  
506 number of taxa. In contrast, the number of calculations in the pruning algorithm only grows  
507 linearly, and therefore trees with thousands of tips can be analyzed (Mitov and Stadler 2019).  
508 Furthermore, even though several methods for dealing with sparse matrices make it possible to  
509 analyze larger numbers of taxa (e.g. Hadfield and Nakagawa 2010),  $\mathbf{C}^*$  has more covariance  
510 entries and is therefore less sparse than  $\mathbf{C}$ ; this again limits matrix-based approaches in  
511 phylogenomic comparative methods.

512

513        Both of our approaches can be extended in multiple ways. While we have only considered  
514 Brownian motion models here, there are multiple other trait models that could be used. The  
515 Ornstein-Uhlenbeck process is a popular model for trait evolution, with estimators available using  
516 both matrix (Hansen 1997; Butler and King 2004; Beaulieu et al. 2012; Rohlf et al. 2014) and  
517 pruning algorithm approaches (FitzJohn 2012; Ho and Ané 2014; Uyeda and Harmon 2014; Mitov  
518 et al. 2020). Additional models for continuous traits include “early burst” (Harmon et al. 2010)  
519 and Lévy (“jump”) processes (Landis and Schraiber 2017). All of these models should be able to  
520 be accommodated by phylogenomic comparative methods. In addition, although we have  
521 described the covariances in our models with a particular set of gene trees in mind, both methods  
522 can be used with any weighted mixture of trees. This means that users do not have to assume a  
523 particular model of species tree evolution (e.g. the multispecies coalescent model) and can even

524 ignore ILS altogether in favor of phylogenetic network models (e.g. Bastide et al. 2018). This  
525 should also allow our approaches to accommodate unequal contributions to trait variation across  
526 individual loci, for example, if some loci are known to be functionally related to the trait of interest  
527 and therefore expected to have mutations of larger effect on average.

528  
529 There are also multiple caveats that come with our proposed approaches, and some  
530 important technical limitations to consider. First, errors in gene tree or species tree specification  
531 might bias inferences. This is especially true if gene trees are being used as inputs, as we require  
532 both accurate and ultrametric trees. Our methods assume that loci controlling trait variation and  
533 the genome at large follow the same distribution of trees; however, if trait loci experience stronger  
534 than average selection, these loci could have proportionally fewer discordant gene trees than the  
535 genomic background ([cite something here?](#)). Gene trees may also be mis-specified due to technical  
536 errors in their estimation. We found that error in gene tree frequencies and branch lengths is  
537 relatively inconsequential for our approaches, under the conditions considered here. Specifying a  
538 set of incorrect gene tree topologies may have more of an effect, but since ILS is expected to  
539 generate all possible topologies with respect to a single branch, we do not expect this to be a  
540 significant issue. Obtaining ultrametric gene trees remains challenging due to variation in rates of  
541 evolution among loci and small amounts of data per locus. Even when species trees are used to  
542 generate gene tree frequencies (i.e. `get_full_matrix`), many coalescent-based methods for inferring  
543 species trees do not estimate tip branch lengths (e.g. Liu et al. 2010; Mirarab et al. 2014), further  
544 limiting accurate inferences (but see Bastide et al. 2018; Hibbins et al. 2020). If there is uncertainty  
545 in the species tree topology or branch lengths, a straightforward solution would be to embed the  
546 approaches used here within a Bayesian framework (e.g. Huelsenbeck et al. 2000; Pagel and  
547 Meade 2006). It is important to note, however, that gene tree discordance is not equivalent to  
548 species tree uncertainty: averaging over each gene tree topology on its own in a Bayesian  
549 framework would simply mean averaging over many incorrect trees. Instead, a proper Bayesian  
550 approach to accommodating discordance would have to sum over a new set of gene trees (or  
551 covariances) for each species tree topology proposed, as was done here with a single topology.

552  
553 A second caveat is that large numbers of taxa make it harder to accurately estimate both  
554 the matrix used in *seastar* and the gene trees used within the pruning algorithm. If gene trees are  
555 predicted from theory, *seastar* calculates  $\mathbf{C}^*$  from the species tree by breaking the tree into triplets.  
556 While this will return approximately correct covariances for all pairs of species, it necessarily  
557 ignores any covariance structures that might only be possible in trees with four or more taxa. The  
558 problem for the pruning algorithm approach could be even worse, as separate gene tree topologies  
559 must be specified: specifying representative gene trees for all possible topologies becomes  
560 prohibitive with more taxa because the number of gene trees grows super-exponentially. Even if  
561 gene trees are estimated from the data, with only a few dozen taxa there are more possible gene  
562 tree topologies than independent loci in a genome. Two solutions suggest ways around these  
563 issues. First, the problems can be somewhat ameliorated by recognizing that it is not the number  
564 of taxa that is the issue, but instead the number of lineages within “knots” (cf. Ané et al. 2007) on  
565 the larger phylogeny that are prone to gene tree discordance. For instance, even in a tree with 100  
566 species, if only three are undergoing ILS, then only three topologies must be considered. Judicious  
567 choices as to the number of different topologies that must be considered in any particular analysis  
568 could save a lot of computational effort. Second, as mentioned in the Methods, one approach that  
569 can be applied to the pruning algorithm method is to sample a limited number of individual gene

570 trees, either directly from the inferred trees or from the multispecies coalescent model applied to  
571 the species tree. Even if we have to sample 100 trees, the likelihood calculations on each are  
572 relatively fast and can be parallelized. Such a sampling scheme will also naturally recapitulate the  
573 degree of discordance associated with every branch in the species tree.

574

575 Throughout our analyses, we found that rate estimates using a single species tree differed  
576 from those accounting for gene trees, even when the level of discordance was very low or zero  
577 (Figure 4A). This result occurs because the two modes of inference are fundamentally different:  
578 even with no discordance, “gene tree” analyses are based on gene tree branch lengths, not species  
579 tree branch lengths. Gene tree branch lengths are always longer than species tree branch lengths  
580 because each pair of lineages is expected to coalesce  $2N$  generations before their time of speciation  
581 (Gillespie and Langley 1979; Edwards and Beerli 2000). These longer gene tree branch lengths  
582 result in higher trait variances in the traits, such that a higher evolutionary rate must be proposed  
583 to explain the same data when using the species tree for analysis. This distinction highlights an  
584 additional challenge for a potential application of our pruning algorithm approach – ancestral state  
585 reconstruction. Because the internal nodes of gene trees—including concordant gene trees—do not  
586 exist at the same moment of time as the internal nodes of species trees, reconstructing ancestral  
587 states at the time of speciation requires knowledge of the contribution of each gene tree branch to  
588 trait evolution at that particular time point. This could be accomplished by the insertion of single-  
589 descendant nodes on gene tree lineages that are concurrent with ancestral nodes on the species  
590 tree. Inferring lineage-specific rate shifts will likewise require that each gene tree branch, or  
591 segment of a gene tree branch, be assigned to specific species tree lineages (cf. Ogilvie et al. 2017).  
592 In general, these considerations highlight the fact that using gene trees in place of a species tree is  
593 a fundamentally different mode of inference, and that standard comparative methods using the  
594 species tree may yield incorrect inferences even if there is no discordance.

595

596 We consistently found that evolutionary rate estimates for tomato floral traits were much  
597 greater using species tree approaches than our gene tree approaches (Figure 6). For the high ILS  
598 triplet, there was even more bias than in the low ILS knot. These results are consistent with a  
599 contribution of gene trees, rather than a single species phylogeny, to variation in these traits. Our  
600 analysis of gene tree error suggests that this result is not simply an artifact of increasing the  
601 specified rate of gene tree discordance, but is the result of biological variation in the floral traits.  
602 Furthermore, our findings have implications for the study of evolutionary rate variation among  
603 clades. For example, imagine that researchers wished to investigate whether the evolutionary rate  
604 of corolla diameter differed between our high ILS and low ILS triplets. Applying standard species  
605 tree methods, they would find that the corolla diameter of the high ILS species evolves at a much  
606 faster rate than in their low ILS counterparts. However, from our results in Figure 6, after  
607 correcting for the contribution of discordant gene trees, this difference disappears and the trait  
608 appears to evolve at approximately the same rate in both clades. This result highlights how  
609 variation in the rate of gene tree discordance among clades is a confounding factor when studying  
610 the evolution of lineage-specific rate shifts.

611

612 An increasingly common finding in phylogenomics is that of rapid and/or highly parallel  
613 trait evolution associated with rapid species radiations (Schluter et al. 1997; Boughman et al. 2005;  
614 Sun et al. 2012; Parins-Fukuchi et al. 2021; Urban et al. 2022). The application of classic  
615 comparative approaches in these systems has suggested that many radiations violate constant-rate

616 Brownian motion models, with more complex models being proposed instead (Simpson 1944;  
617 Blomberg et al. 2003; Freckleton and Harvey 2006). However, adaptive radiations often have very  
618 little time between speciation events, resulting in high rates of gene tree discordance and therefore  
619 high potential for hemiplasy (Pease et al. 2016). Here we have found that apparently higher rates  
620 of trait evolution in rapid radiations may be perfectly consistent with a standard Brownian motion  
621 model with a constant evolutionary rate. In this circumstance, higher apparent rates of evolution  
622 are simply the result of a stronger contribution of discordant gene trees to covariance among  
623 species. Our proposed phylogenomic comparative methods help to address these issues, providing  
624 more accurate evolutionary inferences in systems with high rates of discordance.  
625

## 626 **Acknowledgements**

627

628 We would like to thank Ben Fulton and Jason Bertram for offering helpful programming  
629 and statistical advice in implementing the pruning algorithm approach, as well as David Haak for  
630 sharing floral trait data. Two reviewers provided helpful comments on the manuscript. This work  
631 was supported by the EEB Postdoctoral Fellowship awarded to Mark Hibbins by the Department  
632 of Ecology and Evolutionary Biology at the University of Toronto, as well as National Science  
633 Foundation grant DEB-1936187 awarded to Matthew Hahn.  
634

635

636

637

638

639

640

641

642

643

644

645

646

647

648

649

650

651

652

653

654

655

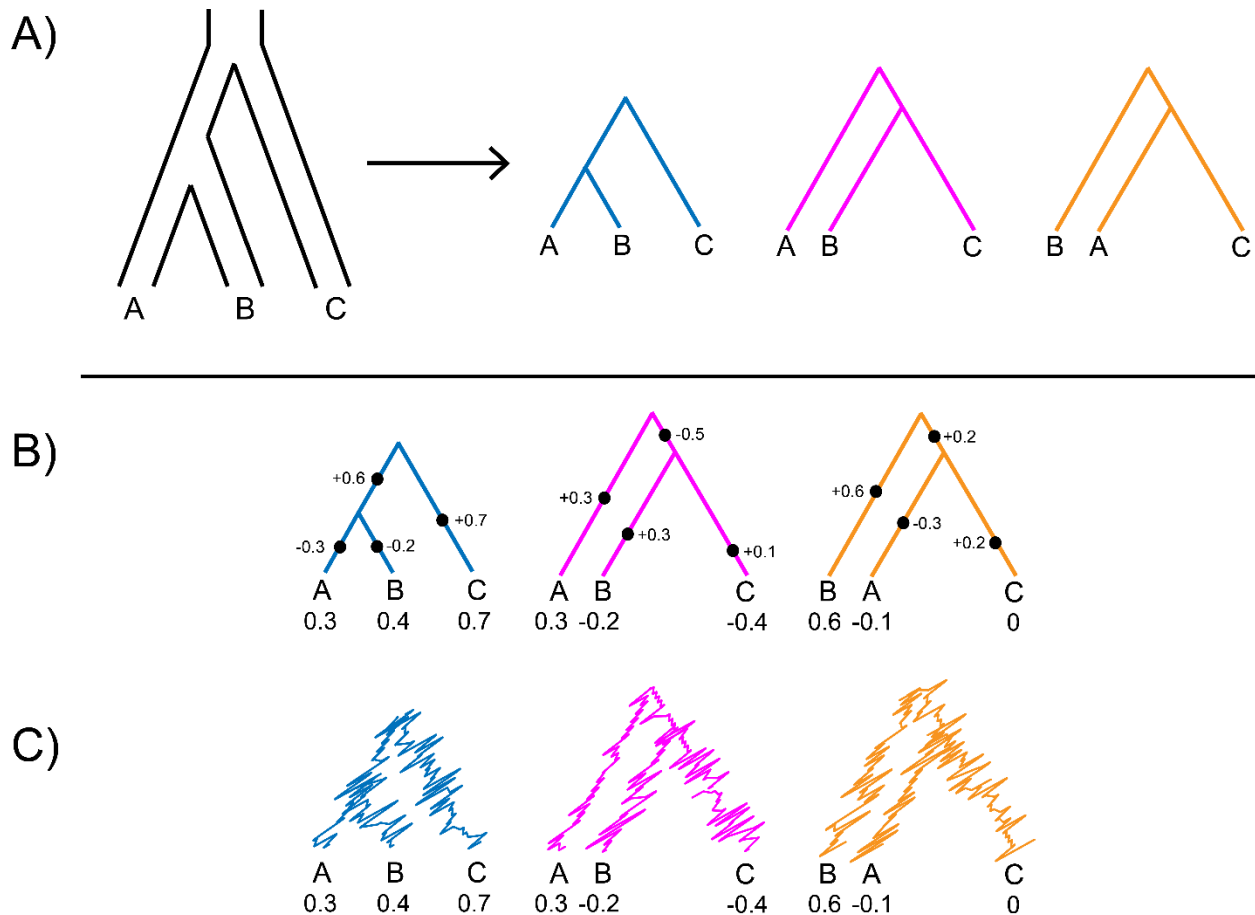
656

657

658

## 659 **Figures**

660

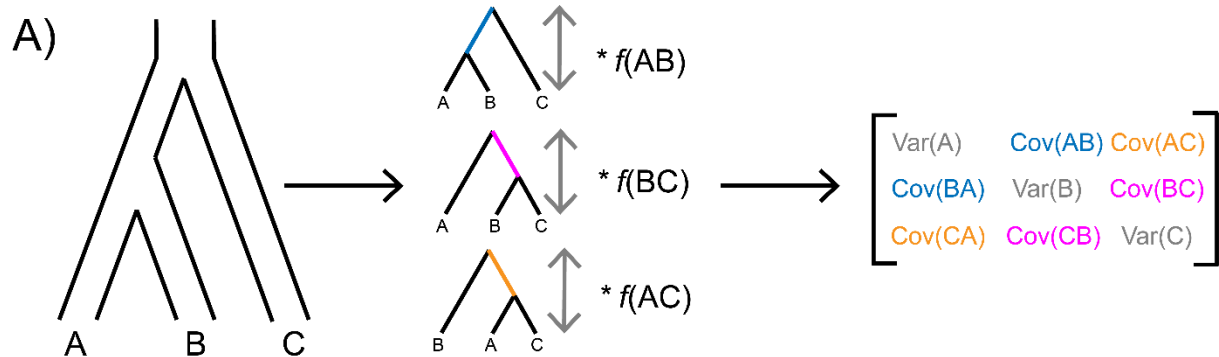


661  
662

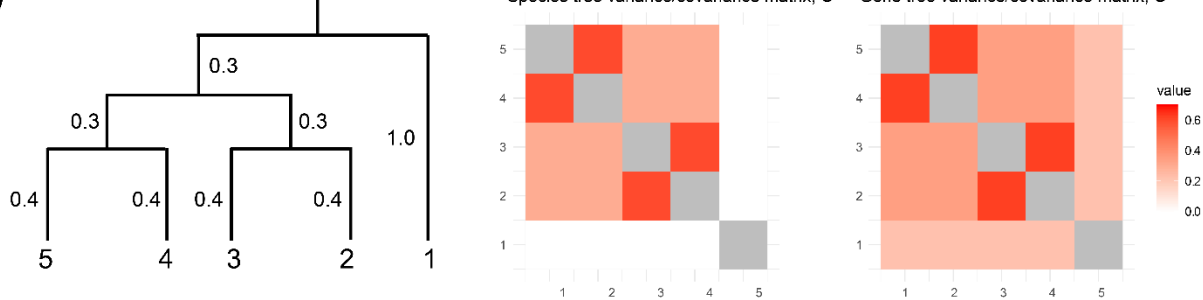
**Figure 1:** Conceptualizing quantitative trait evolution with discordant gene trees. A) Given a species tree (far left), we model gene trees as arising under the multispecies coalescent process. One topology is concordant with the species tree (blue), while the other two possible topologies are discordant (red and yellow). Under ILS these two discordant trees have the same topology and frequency. B) Over the course of evolution, mutations occur at loci that affect quantitative traits, each of which has a topology drawn from the multispecies coalescent process. Mutations on the internal branches of discordant gene trees can introduce shared trait history that is not captured by the species tree. Here we summarize mutations occurring at different loci on a single tree if the loci had the same topology, with each mutation at each locus contributing positively or negatively to the trait value in each species. In the example here, species pairs B-C and A-C might covary in quantitative trait values due to mutations on shared branches in gene trees, despite sharing no common ancestor in the species tree. For example, a mutation on the internal branch of the magenta tree causes species B and C to have more similar trait values. C) Given a large number of mutations and loci, trait evolution over time can be modelled by Brownian motion on each gene tree topology. This stochastic process models the trait value as a random walk over time, with species trait values calculated as the weighted average of the values on each gene tree (Mendes et al. 2018; Hibbins and Hahn 2021).

680  
681  
682  
683

684



B)



685

686

687 **Figure 2:** Inferring the gene tree variance/covariance matrix,  $\mathbf{C}^*$ . A) Gene trees are generated from  
 688 a species tree under the multispecies coalescent process (note that introgression can readily be  
 689 incorporated, but is not shown here for clarity). Each gene tree contributes its internal branch  
 690 length (for covariance terms) and its total height (for variance terms) to  $\mathbf{C}^*$ . The contribution of  
 691 each tree to  $\mathbf{C}^*$  is weighted by its expected or observed frequency, depending on the approach  
 692 taken. Frequencies are denoted as  $f(XY)$ , where X and Y are the taxa sister in the gene tree of  
 693 interest. B) A comparison of  $\mathbf{C}$  and  $\mathbf{C}^*$  for a five-taxon species tree with branch lengths labelled  
 694 in coalescent units (not precisely to scale). Each internal branch has a length of 0.3, corresponding  
 695 to a level of discordance of approximately 50%. This level of discordance means that each clade  
 696 descended from these internal branches (5/4/3/2, 5/4, and 3/2) will be present in ~50% of gene  
 697 trees. The standard phylogenetic covariance matrix,  $\mathbf{C}$ , contains no covariance between species 1  
 698 and the other taxa, because they do not share an internal branch in the species tree. In contrast,  
 699 species 1 covaries with all other species in the tree using  $\mathbf{C}^*$ , because multiple discordant gene  
 700 trees have species 2-5 sharing an internal branch with species 1.

701

702

703

704

705

706

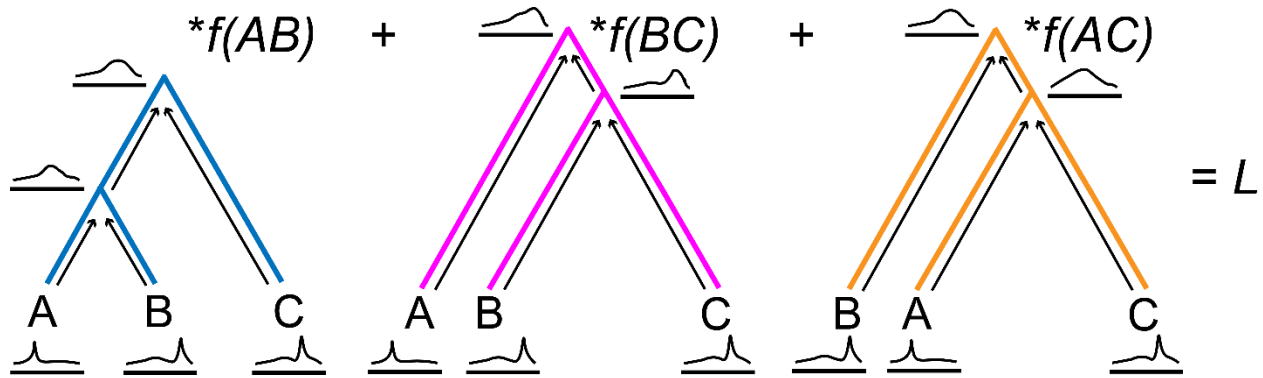
707

708

709

710

711



712

713

714 **Figure 3:** Applying the pruning algorithm to sets of gene trees. In our proposed approach, the  
 715 pruning algorithm (shown as upward arrows) is applied to each individual gene tree to obtain  
 716 character state probabilities at each node (curved lines) up to the root for a quantitative trait. These  
 717 root probabilities are then used to obtain a partial likelihood from each gene tree, which are then  
 718 summed together weighted by the gene tree frequency to obtain the final likelihood.

719

720

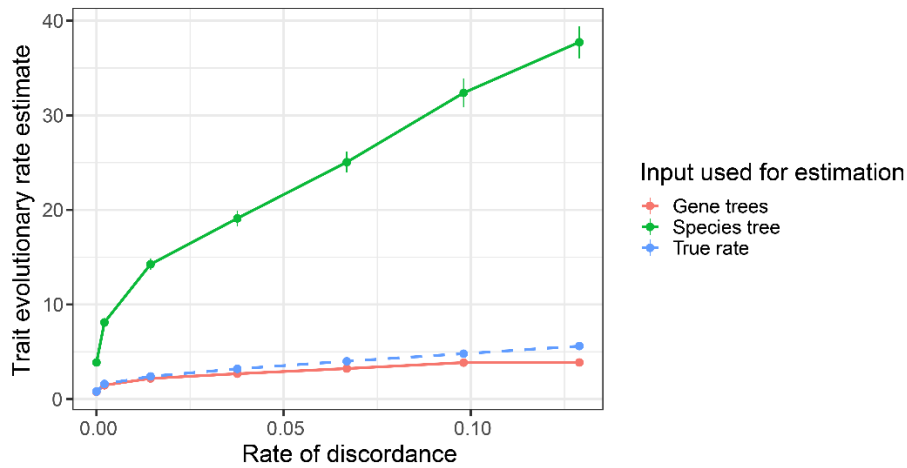
721

722

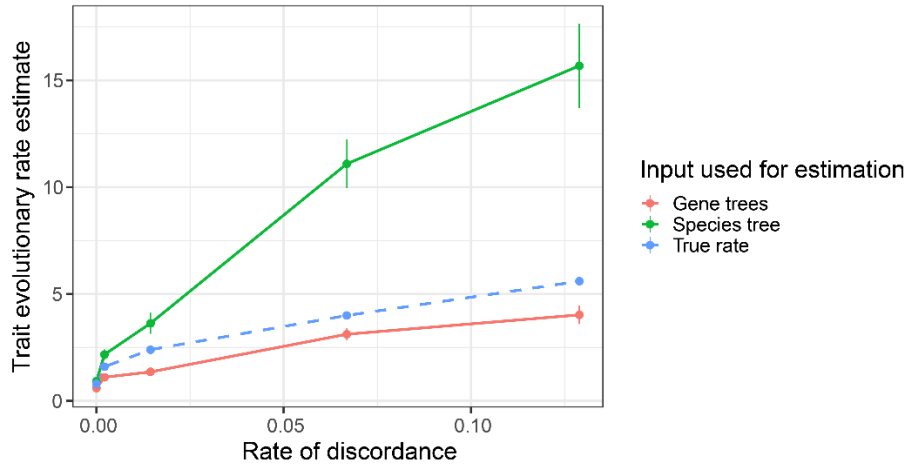
723

724

### A) Covariance matrix method



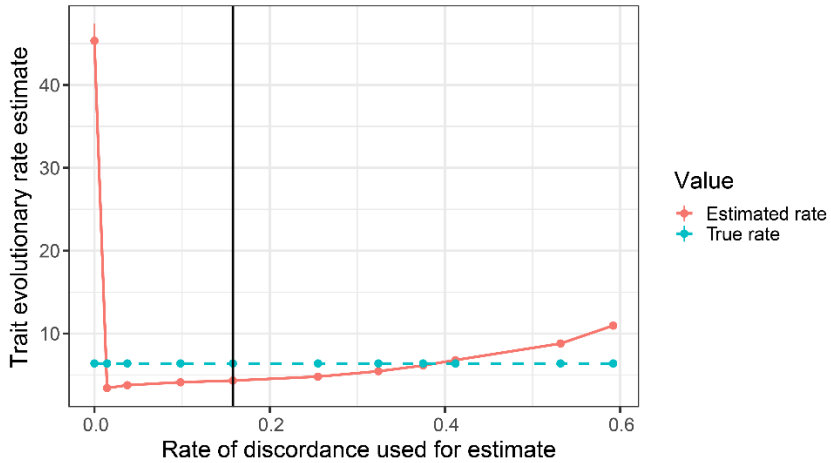
### B) Pruning algorithm method



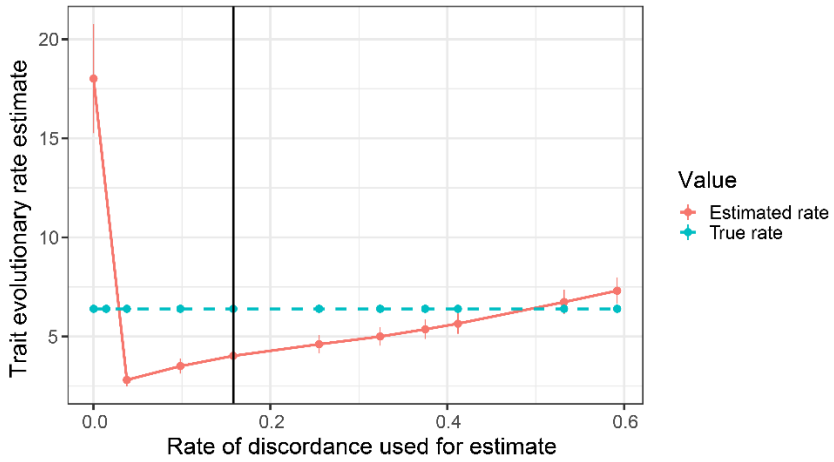
725  
726  
727  
728  
729  
730  
731  
732  
733  
734  
735  
736  
737  
738

**Figure 4:** Phylogenomic comparative methods produce more accurate evolutionary rate estimates. A) Rate estimates obtained using a maximum-likelihood estimator applied to the covariance matrix (equation 5). B) Rate estimates obtained using numerical optimization of the likelihood with the pruning algorithm. In both panels, the green line shows inferences from methods using only the species tree, the red line shows the inferences from methods accounting for gene tree discordance, and the blue dashed line shows the true simulated value of the evolutionary rate. The level of gene tree discordance expected from each simulated species tree (see Supplementary Methods) is shown on the x-axis. Note that panels A and B have different y-axis scales.

A) Covariance matrix method



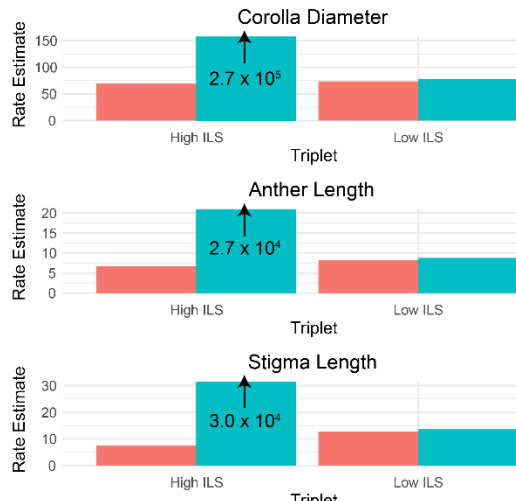
B) Pruning algorithm method



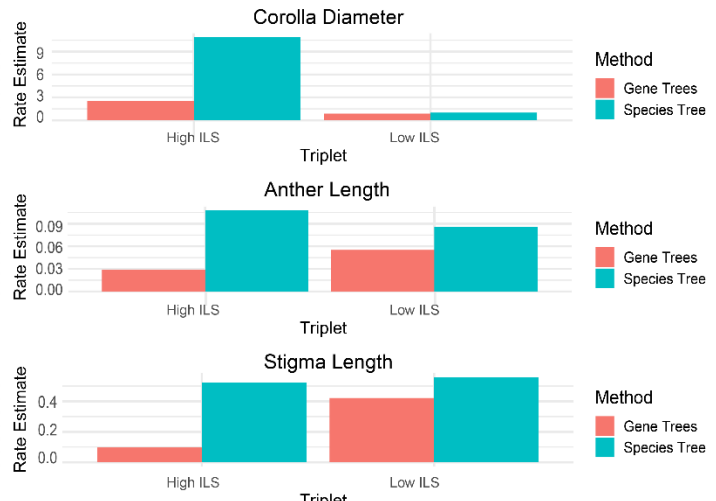
739  
740

741 **Figure 5:** Phylogenomic comparative methods are robust to gene tree estimation error. In both  
742 panels, the solid vertical line denotes the true rate of discordance used to simulate the trait data,  
743 and the horizontal blue line denotes the true evolutionary rate. The x-axis shows the rate of  
744 discordance supplied to each approach when estimating the evolutionary rate from the simulated  
745 data. For a rate of discordance equal to 0, we used the standard species tree inference rather than  
746 gene tree inference. Specifying too much discordance can also cause overestimation of the  
747 evolutionary rate. Note that panels A and B have different y-axis scales.  
748  
749  
750  
751  
752  
753

A) Covariance matrix method (seastaR)



B) Pruning algorithm method

754  
755

756 **Figure 6:** Evolutionary rate estimates for three floral traits in *Solanum* using our newly developed  
 757 approaches (red bars), in comparison to standard species tree methods (blue bars). A) rate estimates  
 758 ( $\sigma^2$ ) obtained using the analytical maximum-likelihood estimator as implemented in our R package  
 759 *seastaR*. In the high ILS triplet, the species tree estimates (blue) go far above the scale of the y-  
 760 axis, so these bars are labelled with an up arrow and the true estimated values for clarity. B) Rate  
 761 estimates ( $\sigma^2$ ) obtained via maximum likelihood optimization using our pruning algorithm  
 762 implementation for calculating likelihoods on gene trees. Note that the values on the y-axes are  
 763 not the same in the two panels.

764  
765  
766  
767  
768  
769  
770  
771  
772  
773  
774  
775  
776  
777  
778  
779  
780  
781  
782  
783  
784  
785

786

787 **References**

788

789 Adams, D. C., & Collyer, M. L. (2018). Multivariate phylogenetic comparative methods:  
 790 evaluations, comparisons, and recommendations. *Systematic Biology*, 67(1), 14-31.  
 791 doi:10.1093/sysbio/syx055

792 Alfaro, M. E., Santini, F., Brock, C., Alamillo, H., Dornburg, A., Rabosky, D. L., . . . Harmon, L.  
 793 J. (2009). Nine exceptional radiations plus high turnover explain species diversity in jawed  
 794 vertebrates. *Proceedings of the National Academy of Sciences of the United States of  
 795 America*, 106(32), 13410-13414. doi:10.1073/pnas.0811087106

796 Ane, C., Larget, B., Baum, D. A., Smith, S. D., & Rokas, A. (2007). Bayesian estimation of  
 797 concordance among gene trees. *Molecular Biology and Evolution*, 24(2), 412-426.  
 798 doi:10.1093/molbev/msl170

799 Avise, J. C., & Robinson, T. J. (2008). Hemiplasy: a new term in the lexicon of phylogenetics.  
 800 *Systematic Biology*, 57(3), 503-507. doi:10.1080/10635150802164587

801 Bastide, P., Solis-Lemus, C., Kriebel, R., William Sparks, K., & Ane, C. (2018). Phylogenetic  
 802 comparative methods on phylogenetic networks with reticulations. *Systematic Biology*,  
 803 67(5), 800-820. doi:10.1093/sysbio/syy033

804 Beaulieu, J. M., Jhueng, D. C., Boettiger, C., & O'Meara, B. C. (2012). Modeling stabilizing  
 805 selection: expanding the Ornstein-Uhlenbeck model of adaptive evolution. *Evolution*,  
 806 66(8), 2369-2383. doi:10.1111/j.1558-5646.2012.01619.x

807 Blomberg, S. P., Garland, T., Jr., & Ives, A. R. (2003). Testing for phylogenetic signal in  
 808 comparative data: behavioral traits are more labile. *Evolution*, 57(4), 717-745.  
 809 doi:10.1111/j.0014-3820.2003.tb00285.x

810 Boucher, F. C., & Demery, V. (2016). Inferring bounded evolution in phenotypic characters from  
 811 phylogenetic comparative data. *Systematic Biology*, 65(4), 651-661.  
 812 doi:10.1093/sysbio/syw015

813 Boughman, J. W., Rundle, H. D., & Schluter, D. (2005). Parallel evolution of sexual isolation in  
 814 sticklebacks. *Evolution*, 59(2), 361-373. Retrieved from  
 815 <https://www.ncbi.nlm.nih.gov/pubmed/15807421>

816 Bryant, D., Bouckaert, R., Felsenstein, J., Rosenberg, N. A., & RoyChoudhury, A. (2012).  
 817 Inferring species trees directly from biallelic genetic markers: bypassing gene trees in a full  
 818 coalescent analysis. *Molecular Biology and Evolution*, 29(8), 1917-1932.  
 819 doi:10.1093/molbev/mss086

820 Butler, M. A., & King, A. A. (2004). Phylogenetic comparative analysis: A modeling approach for  
 821 adaptive evolution. *American Naturalist*, 164(6), 683-695. doi:10.1086/426002

822 Chifman, J., & Kubatko, L. (2014). Quartet inference from SNP data under the coalescent model.

823 *Bioinformatics*, 30(23), 3317-3324. doi:10.1093/bioinformatics/btu530

824 Copetti, D., Burquez, A., Bustamante, E., Charboneau, J. L. M., Childs, K. L., Eguiarte, L. E., . . .  
825 Sanderson, M. J. (2017). Extensive gene tree discordance and hemiplasy shaped the  
826 genomes of North American columnar cacti. *Proceedings of the National Academy of  
827 Sciences of the United States of America*, 114(45), 12003-12008.  
828 doi:10.1073/pnas.1706367114

829 Dagilis, A. J., Peede, D., Coughlan, J. M., Jofre, G. I., D'Agostino, E. R. R., Mavengere, H., . . .  
830 Matute, D. R. (2022). A need for standardized reporting of introgression: Insights from  
831 studies across eukaryotes. *Evolution Letters*, 6(5), 344-357. doi:10.1002/evl3.294

832 De Maio, N., Schlotterer, C., & Kosiol, C. (2013). Linking great apes genome evolution across  
833 time scales using polymorphism-aware phylogenetic models. *Molecular Biology and  
834 Evolution*, 30(10), 2249-2262. doi:10.1093/molbev/mst131

835 De Maio, N., Wu, C. H., O'Reilly, K. M., & Wilson, D. (2015). New routes to phylogeography: a  
836 Bayesian structured coalescent approximation. *PLoS Genetics*, 11(8), e1005421.  
837 doi:10.1371/journal.pgen.1005421

838 Degnan, J. H., & Rosenberg, N. A. (2009). Gene tree discordance, phylogenetic inference and the  
839 multispecies coalescent. *Trends in Ecology and Evolution*, 24(6), 332-340.  
840 doi:10.1016/j.tree.2009.01.009

841 Durand, E. Y., Patterson, N., Reich, D., & Slatkin, M. (2011). Testing for ancient admixture  
842 between closely related populations. *Molecular Biology and Evolution*, 28(8), 2239-2252.  
843 doi:10.1093/molbev/msr048

844 Edelman, N. B., Frandsen, P. B., Miyagi, M., Clavijo, B., Davey, J., Dikow, R. B., . . . Mallet, J.  
845 (2019). Genomic architecture and introgression shape a butterfly radiation. *Science*,  
846 366(6465), 594-599. doi:10.1126/science.aaw2090

847 Edwards, S. V., & Beerli, P. (2000). Perspective: gene divergence, population divergence, and the  
848 variance in coalescence time in phylogeographic studies. *Evolution*, 54(6), 1839-1854.  
849 doi:10.1111/j.0014-3820.2000.tb01231.x

850 Felsenstein, J. (1973). Maximum-likelihood estimation of evolutionary trees from continuous  
851 characters. *American Journal of Human Genetics*, 25(5), 471-492. Retrieved from  
852 <https://www.ncbi.nlm.nih.gov/pubmed/4741844>

853 Felsenstein, J. (1981). Evolutionary trees from DNA-sequences - a maximum-likelihood approach.  
854 *Journal of Molecular Evolution*, 17(6), 368-376. doi:10.1007/Bf01734359

855 Felsenstein, J. (1985). Phylogenies and the comparative method. *American Naturalist*, 125(1), 1-  
856 15. doi:10.1086/284325

857 FitzJohn, R. G. (2012). DiversiTree: comparative phylogenetic analyses of diversification in R.  
858 *Methods in Ecology and Evolution*, 3(6), 1084-1092. doi:10.1111/j.2041-

859 210X.2012.00234.x

860 Fontaine, M. C., Pease, J. B., Steele, A., Waterhouse, R. M., Neafsey, D. E., Sharakhov, I. V., . . .  
861 Besansky, N. J. (2015). Extensive introgression in a malaria vector species complex  
862 revealed by phylogenomics. *Science*, 347(6217), 1258524. doi:10.1126/science.1258524

863 Freckleton, R. P. (2012). Fast likelihood calculations for comparative analyses. *Methods in*  
864 *Ecology and Evolution*, 3(5), 940-947. doi:10.1111/j.2041-210X.2012.00220.x

865 Freckleton, R. P., & Harvey, P. H. (2006). Detecting non-Brownian trait evolution in adaptive  
866 radiations. *PLoS Biology*, 4(11), e373. doi:10.1371/journal.pbio.0040373

867 Garamszegi, L. Z. (2014). *Modern phylogenetic comparative methods and their application in*  
868 *evolutionary biology*. Berlin: Springer.

869 Garland, T., & Ives, A. R. (2000). Using the past to predict the present: Confidence intervals for  
870 regression equations in phylogenetic comparative methods. *American Naturalist*, 155(3),  
871 346-364. doi:10.1086/303327

872 Gillespie, J. H., & Langley, C. H. (1979). Are evolutionary rates really variable? *Journal of*  
873 *Molecular Evolution*, 13(1), 27-34. doi:10.1007/BF01732751

874 Grafen, A. (1989). The phylogenetic regression. *Philosophical Transactions of the Royal Society*  
875 *of London B: Biological Sciences*, 326(1233), 119-157. doi:10.1098/rstb.1989.0106

876 Green, R. E., Krause, J., Briggs, A. W., Maricic, T., Stenzel, U., Kircher, M., . . . Paabo, S. (2010).  
877 A draft sequence of the Neandertal genome. *Science*, 328(5979), 710-722.  
878 doi:10.1126/science.1188021

879 Guerrero, R. F., & Hahn, M. W. (2018). Quantifying the risk of hemiplasy in phylogenetic  
880 inference. *Proceedings of the National Academy of Sciences of the United States of*  
881 *America*, 115(50), 12787-12792. doi:10.1073/pnas.1811268115

882 Haak, D. C., Ballenger, B. A., & Moyle, L. C. (2014). No evidence for phylogenetic constraint on  
883 natural defense evolution among wild tomatoes. *Ecology*, 95(6), 1633-1641.  
884 doi:10.1890/13-1145.1

885 Hadfield, J. D. (2010). MCMC methods for multi-response generalized linear mixed models: the  
886 MCMCglmm R package. *Journal of Statistical Software*, 33(2), 1-22.  
887 doi:10.18637/jss.v033.i02

888 Hadfield, J. D., & Nakagawa, S. (2010). General quantitative genetic methods for comparative  
889 biology: phylogenies, taxonomies and multi-trait models for continuous and categorical  
890 characters. *Journal of Evolutionary Biology*, 23(3), 494-508. doi:10.1111/j.1420-  
891 9101.2009.01915.x

892 Hahn, M. W., De Bie, T., Stajich, J. E., Nguyen, C., & Cristianini, N. (2005). Estimating the tempo  
893 and mode of gene family evolution from comparative genomic data. *Genome Research*,

894 15(8), 1153-1160. doi:10.1101/gr.3567505

895 Hahn, M. W., & Nakhleh, L. (2016). Irrational exuberance for resolved species trees. *Evolution*,  
896 70(1), 7-17. doi:10.1111/evo.12832

897 Hansen, T. F. (1997). Stabilizing selection and the comparative analysis of adaptation. *Evolution*,  
898 51(5), 1341-1351. doi:10.1111/j.1558-5646.1997.tb01457.x

899 Harmon, L. J., Losos, J. B., Jonathan Davies, T., Gillespie, R. G., Gittleman, J. L., Bryan Jennings,  
900 W., . . . Mooers, A. O. (2010). Early bursts of body size and shape evolution are rare in  
901 comparative data. *Evolution*, 64(8), 2385-2396. doi:10.1111/j.1558-5646.2010.01025.x

902 Harvey, P. H., & Pagel, M. (1991). *The comparative method in evolutionary biology*. Oxford:  
903 Oxford University Press.

904 Hibbins, M. S., Gibson, M. J., & Hahn, M. W. (2020). Determining the probability of hemiplasy  
905 in the presence of incomplete lineage sorting and introgression. *eLife*, 9.  
906 doi:10.7554/eLife.63753

907 Hibbins, M. S., & Hahn, M. W. (2021). The effects of introgression across thousands of  
908 quantitative traits revealed by gene expression in wild tomatoes. *PLoS Genetics*, 17(11),  
909 e1009892. doi:10.1371/journal.pgen.1009892

910 Hiscott, G., Fox, C., Parry, M., & Bryant, D. (2016). Efficient recycled algorithms for quantitative  
911 trait models on phylogenies. *Genome Biology and Evolution*, 8(5), 1338-1350.  
912 doi:10.1093/gbe/evw064

913 Ho, L., & Ane, C. (2014). A linear-time algorithm for Gaussian and non-Gaussian trait evolution  
914 models. *Systematic Biology*, 63(3), 397-408. doi:10.1093/sysbio/syu005

915 Housworth, E. A., Martins, E. P., & Lynch, M. (2004). The phylogenetic mixed model. *American  
916 Naturalist*, 163(1), 84-96. doi:10.1086/380570

917 Hudson, R. R. (1983). Testing the constant-rate neutral allele model with protein sequence data.  
918 *Evolution*, 37(1), 203-217. doi:10.1111/j.1558-5646.1983.tb05528.x

919 Huelsenbeck, J. P., Rannala, B., & Masly, J. P. (2000). Accommodating phylogenetic uncertainty  
920 in evolutionary studies. *Science*, 288(5475), 2349-2350.  
921 doi:10.1126/science.288.5475.2349

922 Landis, M. J., & Schraiber, J. G. (2017). Pulsed evolution shaped modern vertebrate body sizes.  
923 *Proceedings of the National Academy of Sciences of the United States of America*, 114(50),  
924 13224-13229. doi:10.1073/pnas.1710920114

925 Liu, L., Yu, L., & Edwards, S. V. (2010). A maximum pseudo-likelihood approach for estimating  
926 species trees under the coalescent model. *BMC Evolutionary Biology*, 10, 302.  
927 doi:10.1186/1471-2148-10-302

928 Mallet, J., Besansky, N., & Hahn, M. W. (2016). How reticulated are species? *BioEssays*, 38(2),  
929 140-149. doi:10.1002/bies.201500149

930 Martins, E. P., & Hansen, T. F. (1996). The statistical analysis of interspecific data: a review and  
931 evaluation of phylogenetic comparative methods. In E. P. Martins (Ed.), *Phylogenies and*  
932 *the comparative method in animal behavior*. New York: Oxford University Press.

933 Mendes, F. K., Fuentes-Gonzalez, J. A., Schraiber, J. G., & Hahn, M. W. (2018). A multispecies  
934 coalescent model for quantitative traits. *eLife*, 7. doi:10.7554/eLife.36482

935 Mendes, F. K., & Hahn, M. W. (2016). Gene tree discordance causes apparent substitution rate  
936 variation. *Systematic Biology*, 65(4), 711-721. doi:10.1093/sysbio/syw018

937 Mendes, F. K., Vanderpool, D., Fulton, B., & Hahn, M. W. (2020). CAFE 5 models variation in  
938 evolutionary rates among gene families. *Bioinformatics*, 36(23), 5516-5518.  
939 doi:10.1093/bioinformatics/btaa1022

940 Mirarab, S., Reaz, R., Bayzid, M. S., Zimmermann, T., Swenson, M. S., & Warnow, T. (2014).  
941 ASTRAL: genome-scale coalescent-based species tree estimation. *Bioinformatics*, 30(17),  
942 i541-548. doi:10.1093/bioinformatics/btu462

943 Mitov, V., Bartoszek, K., Asimomitis, G., & Stadler, T. (2020). Fast likelihood calculation for  
944 multivariate Gaussian phylogenetic models with shifts. *Theoretical Population Biology*,  
945 131, 66-78. doi:10.1016/j.tpb.2019.11.005

946 Mitov, V., & Stadler, T. (2019). Parallel likelihood calculation for phylogenetic comparative  
947 models: The SPLITT C++ library. *Methods in Ecology and Evolution*, 10(4), 493-506.  
948 doi:10.1111/2041-210x.13136

949 Nelder, J. A., & Mead, R. (1965). A simplex-method for function minimization. *Computer*  
950 *Journal*, 7(4), 308-313. doi:10.1093/comjnl/7.4.308

951 Novikova, P. Y., Hohmann, N., Nizhynska, V., Tsuchimatsu, T., Ali, J., Muir, G., . . . Nordborg,  
952 M. (2016). Sequencing of the genus *Arabidopsis* identifies a complex history of  
953 nonbifurcating speciation and abundant trans-specific polymorphism. *Nature Genetics*,  
954 48(9), 1077-1082. doi:10.1038/ng.3617

955 Ogilvie, H. A., Bouckaert, R. R., & Drummond, A. J. (2017). StarBEAST2 brings faster species  
956 tree inference and accurate estimates of substitution rates. *Molecular Biology and*  
957 *Evolution*, 34(8), 2101-2114. doi:10.1093/molbev/msx126

958 O'Meara, B. C., Ane, C., Sanderson, M. J., & Wainwright, P. C. (2006). Testing for different rates  
959 of continuous trait evolution using likelihood. *Evolution*, 60(5), 922-933. Retrieved from  
960 <https://www.ncbi.nlm.nih.gov/pubmed/16817533>

961 Pagel, M. (1999). Inferring the historical patterns of biological evolution. *Nature*, 401(6756), 877-  
962 884. doi:10.1038/44766

963 Pagel, M., & Meade, A. (2006). Bayesian analysis of correlated evolution of discrete characters  
964 by reversible-jump Markov chain Monte Carlo. *American Naturalist*, 167(6), 808-825.  
965 doi:10.1086/503444

966 Pamilo, P., & Nei, M. (1988). Relationships between gene trees and species trees. *Molecular  
967 Biology and Evolution*, 5(5), 568-583. doi:10.1093/oxfordjournals.molbev.a040517

968 Paradis, E., & Schliep, K. (2019). ape 5.0: an environment for modern phylogenetics and  
969 evolutionary analyses in R. *Bioinformatics*, 35(3), 526-528.  
970 doi:10.1093/bioinformatics/bty633

971 Parins-Fukuchi, C., Stull, G. W., & Smith, S. A. (2021). Phylogenomic conflict coincides with  
972 rapid morphological innovation. *Proceedings of the National Academy of Sciences of the  
973 United States of America*, 118(19). doi:10.1073/pnas.2023058118

974 Patterson, N., Moorjani, P., Luo, Y., Mallick, S., Rohland, N., Zhan, Y., . . . Reich, D. (2012).  
975 Ancient admixture in human history. *Genetics*, 192(3), 1065-1093.  
976 doi:10.1534/genetics.112.145037

977 Pease, J. B., Haak, D. C., Hahn, M. W., & Moyle, L. C. (2016). Phylogenomics reveals three  
978 sources of adaptive variation during a rapid radiation. *PLoS Biology*, 14(2), e1002379.  
979 doi:10.1371/journal.pbio.1002379

980 Pennell, M. W., Eastman, J. M., Slater, G. J., Brown, J. W., Uyeda, J. C., FitzJohn, R. G., . . .  
981 Harmon, L. J. (2014). geiger v2.0: an expanded suite of methods for fitting  
982 macroevolutionary models to phylogenetic trees. *Bioinformatics*, 30(15), 2216-2218.  
983 doi:10.1093/bioinformatics/btu181

984 Pollard, D. A., Iyer, V. N., Moses, A. M., & Eisen, M. B. (2006). Widespread discordance of gene  
985 trees with species tree in *Drosophila*: evidence for incomplete lineage sorting. *PLoS  
986 Genetics*, 2(10), e173. doi:10.1371/journal.pgen.0020173

987 Reich, D., Thangaraj, K., Patterson, N., Price, A. L., & Singh, L. (2009). Reconstructing Indian  
988 population history. *Nature*, 461(7263), 489-494. doi:10.1038/nature08365

989 Revell, L. J. (2012). phytools: an R package for phylogenetic comparative biology (and other  
990 things). *Methods in Ecology and Evolution*, 3(2), 217-223. doi:10.1111/j.2041-  
991 210X.2011.00169.x

992 Revell, L. J., & Harmon, L. J. (2008). Testing quantitative genetic hypotheses about the  
993 evolutionary rate matrix for continuous characters. *Evolutionary Ecology Research*, 10(3),  
994 311-331. Retrieved from <Go to ISI>://WOS:000256015000001

995 Revell, L. J., & Harmon, L. J. (2022). *Phylogenetic comparative methods in R*: Princeton  
996 University Press.

997 Rohlf, R. V., Harrigan, P., & Nielsen, R. (2014). Modeling gene expression evolution with an  
998 extended Ornstein-Uhlenbeck process accounting for within-species variation. *Molecular*

999 *Biology and Evolution*, 31(1), 201-211. doi:10.1093/molbev/mst190

1000 Schluter, D., Price, T., Mooers, A. O., & Ludwig, D. (1997). Likelihood of ancestor states in  
1001 adaptive radiation. *Evolution*, 51(6), 1699-1711. doi:10.1111/j.1558-5646.1997.tb05095.x

1002 Schrempf, D., Minh, B. Q., De Maio, N., von Haeseler, A., & Kosiol, C. (2016). Reversible  
1003 polymorphism-aware phylogenetic models and their application to tree inference. *Journal*  
1004 *of Theoretical Biology*, 407, 362-370. doi:10.1016/j.jtbi.2016.07.042

1005 Schrempf, D., Minh, B. Q., von Haeseler, A., & Kosiol, C. (2019). Polymorphism-aware species  
1006 trees with advanced mutation models, bootstrap, and rate heterogeneity. *Molecular Biology*  
1007 *and Evolution*, 36(6), 1294-1301. doi:10.1093/molbev/msz043

1008 Simpson, G. G. (1944). *Tempo and mode in evolution*. New York: Columbia University Press.

1009 Sun, Y., Wang, A., Wan, D., Wang, Q., & Liu, J. (2012). Rapid radiation of *Rheum* (Polygonaceae)  
1010 and parallel evolution of morphological traits. *Molecular Phylogenetics and Evolution*,  
1011 63(1), 150-158. doi:10.1016/j.ympev.2012.01.002

1012 Taylor, S. A., & Larson, E. L. (2019). Insights from genomes into the evolutionary importance and  
1013 prevalence of hybridization in nature. *Nature Ecology & Evolution*, 3(2), 170-177.  
1014 doi:10.1038/s41559-018-0777-y

1015 Urban, S., Gerwin, J., Hulsey, C. D., Meyer, A., & Kratochwil, C. F. (2022). The repeated  
1016 evolution of stripe patterns is correlated with body morphology in the adaptive radiations  
1017 of East African cichlid fishes. *Ecology and Evolution*, 12(2), e8568. doi:10.1002/ece3.8568

1018 Uyeda, J. C., & Harmon, L. J. (2014). A novel Bayesian method for inferring and interpreting the  
1019 dynamics of adaptive landscapes from phylogenetic comparative data. *Systematic Biology*,  
1020 63(6), 902-918. doi:10.1093/sysbio/syu057

1021 Vanderpool, D., Minh, B. Q., Lanfear, R., Hughes, D., Murali, S., Harris, R. A., . . . Hahn, M. W.  
1022 (2020). Primate phylogenomics uncovers multiple rapid radiations and ancient  
1023 interspecific introgression. *PLoS Biology*, 18(12), e3000954.  
1024 doi:10.1371/journal.pbio.3000954

1025 Wang, Y., Cao, Z., Ogilvie, H. A., & Nakhleh, L. (2021). Phylogenomic assessment of the role of  
1026 hybridization and introgression in trait evolution. *PLoS Genetics*, 17(8), e1009701.  
1027 doi:10.1371/journal.pgen.1009701

1028 White, M. A., Ane, C., Dewey, C. N., Larget, B. R., & Payseur, B. A. (2009). Fine-scale  
1029 phylogenetic discordance across the house mouse genome. *PLoS Genetics*, 5(11),  
1030 e1000729. doi:10.1371/journal.pgen.1000729

1031 Wu, M., Kostyun, J. L., Hahn, M. W., & Moyle, L. C. (2018). Dissecting the basis of novel trait  
1032 evolution in a radiation with widespread phylogenetic discordance. *Molecular Ecology*,  
1033 27(16), 3301-3316. doi:10.1111/mec.14780

1034 Zhang, C., Rabiee, M., Sayyari, E., & Mirarab, S. (2018). ASTRAL-III: polynomial time species  
1035 tree reconstruction from partially resolved gene trees. *BMC Bioinformatics*, 19(Suppl 6),  
1036 153. doi:10.1186/s12859-018-2129-y

1037